Electronic and second-order nonlinear optical properties of conformationally locked benzylideneanilines and biphenyls. The effect of conformation on the first hyperpolarizability

Cornelis A. van Walree,[a] Adriaan W. Maarsman,[a] Albert W. Marsman,[a] Marinus C. Flipse,[b] Leonardus W. Jenneskens,*[,a] Wilberth J. J. Smeets[c] and Anthony L. Spek[c]

[a] *Debye Institute, Department of Physical Organic Chemistry, Utrecht University, Padualaan 8, 3584 CH Utrecht, The Netherlands*
[b] *Akzo Nobel Central Research, PO Box 9300, 6800 SB Arnhem, The Netherlands*
[c] *Bijvoet Center for Biomolecular Research, Department of Crystal and Structural Chemistry, Utrecht University, Padualaan 8, 3584 CH Utrecht, The Netherlands*

The first hyperpolarizability β and electronic properties of *N*,*N*-dimethylamine and/or nitro-substituted benzylideneanilines and biphenyls are compared with those of conformationally locked model compounds, *viz*. identically substituted 2-phenyl-3,3-dimethyl-3*H*-indoles and fluorenes, respectively. Although PM3 semi-empirical calculations indicate that a small to moderate increase in β can be achieved by locking the π-systems in a planar conformation, experimental results show that the actual gain is either small or negligible. This mainly finds its origin in relatively narrow electronic absorption bands of the conformationally locked compounds, which are related to their rigidity. Moreover, single crystal X-ray structures of the donor–acceptor substituted 3*H*-indoles demonstrate that the presence of a saturated bridge does not necessarily lead to a more planar structure. Furthermore, it is shown that the difference in β of the two *N*,*N*-dimethylamino-nitro-substituted benzylideneaniline isomers is of electronic rather than of conformational origin.

Introduction

The design of molecules with large first hyperpolarizabilities β and the elucidation of structure–activity relationships are important issues for the development of organic materials with large second-order nonlinear optical responses. Although it has been recognized that impressive first hyperpolarizabilities can be obtained for donor–acceptor substituted π-conjugated compounds which possess low-lying charge transfer (CT) states,[1,2] a considerable structural variation is possible within this class of compounds. Hence, the effects of structural parameters such as donor and acceptor strengths[3–10] and both the electronic structure[4–7,9,11] and length[4–6,10,12] of the conjugation path on β have been the subject of numerous experimental and theoretical investigations.[13,14] However, the role of planarity of the π-system has been addressed on a relatively small number of occasions. Barzoukas and co-workers investigated the dependence of β on the conformation of donor–acceptor substituted diphenylacetylenes and stilbenes and concluded that experimental hyperpolarizabilities correspond to a weighted average of the values of rotational conformers.[15,16] Furthermore, differences in nonlinear optical activity between biphenyls and fluorenes have been discussed in terms of planarity of the π-system.[6,17] The importance of π-system planarity is indicated by large optical nonlinearities found for planar-locked polyene dyes.[18]

Prompted by our investigation on the nonlinear optical properties of benzylideneanilines[19] we were interested in studying the effect of π-system planarity on the magnitude of β. Benzylideneanilines (compound types **4** and **5**, Scheme 1) as well as biphenyls (compound type **6**) are suitable for such a study, since their π-systems are, depending on the substituents, usually not planar. In the benzylideneanilines twisting of the π-system originates from a steric interaction of the azomethine proton (−CH=N−) and the *ortho* positioned protons in the aniline ring

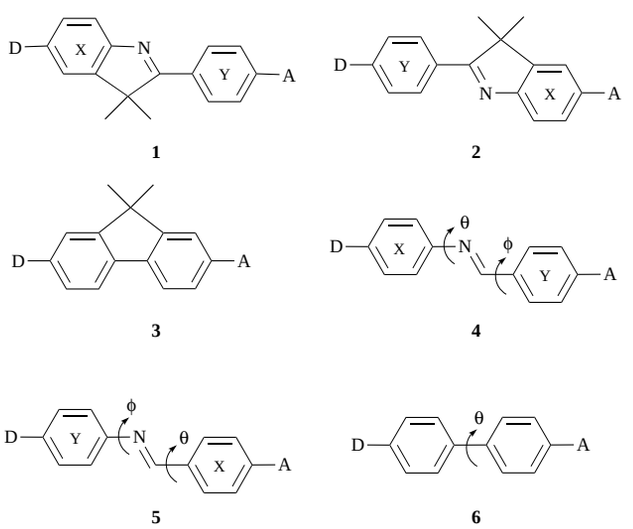

	D	A
1–6D	Me_2N	H
1–6A	H	NO_2
1–6DA	Me_2N	NO_2

Scheme 1

(X) and the possibility of the azomethine nitrogen lone pair (which possesses electron-donating character) to interact with the π-system upon twisting.[20,21] It has been shown that the latter interaction can have a dramatic impact on the optical properties of π-conjugated donor–acceptor systems.[22,23] The main cause for the non-coplanar geometry of biphenyls is steric hindrance between protons positioned *ortho* to the phenyl–phenyl

Table 1 PM3 calculated heats of formation ΔH_f°, ground state dipole moments μ_{calc}, ionization potentials E_i and hyperpolarizabilities β_μ as a function of twist angles θ and φ

		4DA				**5DA**				**6DA**			
θ[a]	φ[a]	ΔH_f°[b]	μ_{calc}/D	E_i/eV	$\beta_\mu/10^{-30}$ esu[c]	ΔH_f°[b]	μ_{calc}/D	E_i/eV	$\beta_\mu/10^{-30}$ esu[c]	ΔH_f°[b]	μ_{calc}/D	E_i/eV	$\beta_\mu/10^{-30}$ esu[c]
0	0	56.7	8.00	8.61	26.6	56.4	7.62	8.64	36.3	34.4	7.45	8.67	23.7
30	0	57.0	7.87	8.59	21.7	56.3	7.72	8.64	33.8	35.4	7.34	8.69	20.3
60	0	57.4	7.50	8.57	10.9	55.9	7.85	8.68	29.5	35.4	7.03	8.73	12.1
90	0	57.9	7.29	8.54	3.7	56.0	7.95	8.70	27.7	35.9	6.89	8.76	7.4
0	30	57.0	7.96	8.62	24.0	56.8	7.24	8.64	31.0				
0	60	57.6	7.93	8.65	17.4	57.9	6.71	8.66	18.5				
0	90	58.1	7.92	8.66	13.9	57.8	6.85	8.70	14.5				

[a] θ and φ are defined in Scheme 1. [b] In kcal mol^{-1} (1 cal = 4.184 J). [c] 1 esu = 1 cm^5 s C^{-1} = 3.71 × 10^{-21} C^3 m^3 J^{-2}.

bond. Thus, benzylideneanilines are preferably twisted around θ and biphenyls are twisted around the phenyl–phenyl bond (θ, Scheme 1). The factors inducing twisting of the π-system compete with loss in resonance energy and the partial double bond character of the azomethine–phenylene and phenyl–phenyl bonds (caused by admixture of quinoid states), which favour a planar conformation.

Planar analogues for biphenyls and benzylideneanilines are fluorenes (compound type **3**) and 2-phenyl-3,3-dimethyl-3*H*-indoles (compound types **1** and **2**), respectively. Note that the presence of the 3-methyl groups in the 3*H*-indoles is necessary since protons at these positions will induce tautomerization to the corresponding 2-phenylindoles.[24] Hence, in the present study the second-order nonlinear optical properties of *N*,*N*-dimethylamino- and/or nitro-substituted 3*H*-indoles and benzylideneanilines and *N*,*N*-dimethylamino- and/or nitro-substituted fluorenes and biphenyls are compared. The monosubstituted Dπ and πA compounds are taken into consideration because they in particular are known to be severely twisted (*vide infra*) and knowledge of their properties may contribute to the understanding of the hyperpolarizabilities of the donor–acceptor (DπA) compounds. In addition to first hyperpolarizabilities, properties such as electronic transitions, redox potentials and structural features of the compounds are discussed. A study of the geometrically well defined planar-locked compounds has the additional advantage that interpretation of results may be facilitated, so that it can contribute to a better understanding of structure–property relationships.

Results and discussion

Theoretical considerations

The effect of introduction of non-planarity as a result of rotation around twist angles θ and φ on the heat of formation ΔH_f°, the ionization potential E_i and the projection of the hyperpolarizability along the dipole moment β_μ of the donor–acceptor substituted compounds **4DA**, **5DA** and **6DA** has been investigated by use of PM3 semi-empirical calculations. The results demonstrate that for **4DA** rotation around both θ and φ results in a gradual increase in ΔH_f° (Table 1). In **5DA** ΔH_f° is raised with increasing φ, but for rotation along θ ΔH_f° decreases with a shallow minimum near θ = 30–60°. Otherwise than reported by others[25] the PM3 method thus predicts a conformationally twisted structure for this compound. For biphenyl **6DA** the planar geometry is calculated to be the most stable conformation.

Energy differences between the most stable and other conformations are however rather small, *i.e.* in the same order of magnitude as the Boltzmann factor RT (RT = 0.6 kcal mol^{-1} at 298 K). Hence, it is appropriate to assume that all DπA compounds are subject to a conformational equilibrium.[15,16] Based on the ΔH_f° values for the several conformations it is expected that preferential twist angles roughly fall in the range of $\theta \approx$ 0–30° and $\varphi \approx$ 0–30° for **4DA**, $\theta \approx$ 0–90° and $\varphi \approx$ 0–30° for **5DA** and $\theta \approx$ 0–60° for **6DA**.

Consequently, the molecular structure of **4DA** is calculated to be more or less planar, whereas the aniline ring of **5DA** is severely twisted out of the C–N=C–C plane. These results are in accordance with previously reported experimental[26–28] and theoretical data[29,30] and crystal structures[31] of **4DA** and **5DA** (*vide infra*). In biphenyl **6DA** a planar conformation is favoured as well, in agreement with the planar single crystal X-ray structure of 4-amino-4′-nitrobiphenyl.[32] However, based on electronic absorption data θ was estimated to be 18° in solution,[6] which emphasizes the importance of packing effects in the solid state structures of biphenyls. For example, biphenyl itself is planar in the solid state, whereas in the gas phase and in solution torsion angles of 43 and 25°, respectively, were found.[33] These data seem to be in line with the outcome of the PM3 calculations that rotation around θ in **6DA** occurs readily.

Concerning geometries of the monosubstituted Dπ and πA compounds it has been deduced from NMR data that **4D**, **4A** and **5A** are not planar.[26,27,34] PCILO calculations revealed torsion angles of 30° in **4D**, **5D** and **4A** and of 60° in **5A**.[35] The dihedral angle θ between the phenyl rings in 4-nitrobiphenyl **6A** was shown to be 33°, both in the crystalline state and in the gas phase.[36]

According to the PM3 calculations, ionization potentials E_i of the donor–acceptor substituted compounds are weakly affected by rotation.† It thus appears that the conformation of the compounds and a possible interaction of the azomethine lone pair with the π-system have a small effect on the electron releasing ability of the dimethylaniline donor. Although effects are small, ionization potentials tend to increase with θ and φ, reflecting gradual localization of electron density on the dimethylaminophenyl moieties. However, in **4DA** the calculations suggest that E_i is reduced with increasing θ.‡

Along all twist angles the hyperpolarizability β_μ is lowered, reflecting the loss in conjugation efficiency. The decrease in β_μ appears to be quantitatively directed by the magnitude of the twist angles, since excellent linear relations between β_μ and either $\cos^2\theta$ or $\cos^2\varphi$ are found (Table 2). The parameters of the regression analyses, the slope ρ and the intercept b, provide information about the sensitivity of the hyperpolarizability to rotation and interactions between the substituents and the bridge. For **5DA** a weak dependence of β_μ on θ is found. This can be attributed to an increased CT interaction of the lone pair of the azomethine nitrogen atom with the nitro group upon twisting around θ, which partially compensates the loss in dimethylamino–nitro CT interaction. This interaction also accounts for the large residual β_μ at θ = 90°, where the dimethylaminophenyl and nitrophenyl π-MOs are fully decoupled. Rotation around φ

† PM3 calculated electron affinities, as estimated from LUMO energies, are unreliable so that an analysis of torsion effects is hampered.

‡ The decrease of E_i of **4DA** with increasing θ is possibly explained by a synergistic effect of the electron-donating abilities of the dimethylamino and azomethine nitrogen atoms, since the lone pair on the azomethine nitrogen atom comes into conjugation with the dimethylamino group upon rotation along θ.

Table 2 Linear regression analysis of β_μ *vs.* twist angles θ and φ ($\beta_\mu = \rho \cos^2 \theta + b$ or $\beta_\mu = \rho \cos^2 \varphi + b$) for compounds **4DA**, **5DA** and **6DA**

	Angle	$\rho/10^{-30}$ esu	$b/10^{-30}$ esu	r^a
4DA	θ	22.6	4.4	0.997
4DA	φ	12.8	14.1	0.999
5DA	θ	8.6	27.5	0.998
5DA	φ	22.5	13.8	0.998
6DA	θ	16.3	7.7	0.998

[a] Correlation coefficient.

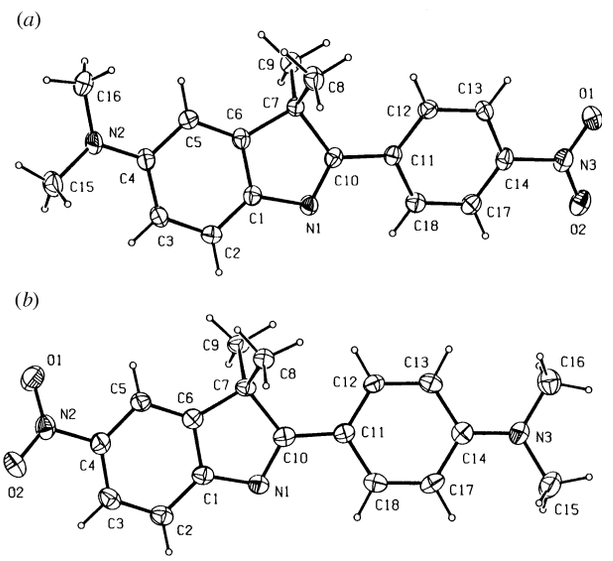

Fig. 1 Thermal motion ellipsoid plots (50% probability) of the X-ray structures of (*a*) **1DA** and (*b*) **2DA** with the adopted atom labelling

in **5DA** has a much stronger reducing effect on the hyperpolarizability. For **4DA** twisting around φ results in the weaker decrease of β_μ, and, hence, leaves the largest residual β_μ; at $\theta = 90°$ a very small β_μ of 3.7×10^{-30} esu is left. It thus appears that in **4DA** the hyperpolarizability associated with the Dπ part is larger than the hyperpolarizability associated with the πA part. The residual hyperpolarizabilities in **5DA** are however comparable to or larger than those in **4DA**. Accordingly, the electronic interactions of the azomethine bridge, such as orientated in **5DA**, with the donors and acceptors are more beneficial for the nonlinear optical activity in fully twisted structures. This is consistent with trends in both experimental and calculated hyperpolarizabilities of monosubstituted benzylideneanilines.[19]

In biphenyl **6DA** the decrease of β_μ with θ is moderate. At $\theta = 90°$ β_μ is small, which must be ascribed to the absence of a redox active bridge. Nevertheless, the hyperpolarizability along the length axis, 7.7×10^{-30} esu exceeds the sum of PM3 calculated hyperpolarizabilities of *N*,*N*-dimethylaniline (3.2×10^{-30} esu) and nitrobenzene (0.02×10^{-30} esu) along their length axes. This suggests the presence of a donor–acceptor interaction at $\theta = 90°$, which has to be operative *via* the σ-system.

In summary, PM3 calculations predict a close to planar geometry for **4DA** and **6DA** but indicate as well that deviations from planarity can occur. The first hyperpolarizability decreases upon twisting. This decrease is however not very pronounced for not too large twist angles, so that a moderate gain in β should be achieved by fixation of these compounds in a planar conformation. Benzylideneaniline **5DA** appears to be severely twisted. Although the decrease of β_μ with θ in this compound is relatively small, the effect of fixation on the hyperpolarizability is anticipated to parallel that in **4DA** and **6DA**, since it is θ that is large in **5DA**. On the other hand, calculated hyperpolarizabilities β_μ of the planar model compounds, which are 25.1 (**1DA**), 33.9 (**2DA**) and 21.6×10^{-30} esu (**3DA**), respectively, are systematically smaller than those of the planar, unfixed compounds. This finding suggests that structural features other than planarity are of significance as well, as is shown below.

X-Ray structures of donor-acceptor substituted 3*H*-indoles

The X-ray structures of benzylideneanilines **4DA** and **5DA** have been reported previously by Nakai *et. al.*[31] They showed that the aniline rings (X, Scheme 1) are twisted out of the −C=N− plane by 9.2° in **4DA** and by 41.5 and 49.0° in **5DA**, where the unit cell contains two molecules. The twist angles for the benzylidene rings (Y) are 4.1° (**4DA**) and 11.4° (**5DA**). The geometry of **4DA** is thus nearly planar, while **5DA** possesses a nonplanar conformation. In the X-ray structures of 3*H*-indoles **1DA** and **2DA** (Fig. 1, Tables 3 and 4) the phenyl groups X are coplanar with the azomethine bridge. The five-membered rings are essentially planar; in **1DA**, torsion angles do not exceed 3.4° in this ring system, in **2DA** they are less than 2.5°. The angles between the planes N(1)−C(1)−C(6)−C(7)−C(10) and C(1)−C(2)−C(3)−C(4)−C(5)−C(6) are 3.4(1)° (**1DA**) and 3.0(1)° (**2DA**), respectively. In contrast, the phenylene groups Y in the 3*H*-indoles are more twisted with respect to the azomethine bridge than the phenylene groups in the benzylideneanilines. The torsion angles to the plane of the five-membered rings of these rings amount to 17.8(1)° in **1DA** and 15.0(1)° in **2DA**.

We attribute the higher degree of twisting of ring Y in the 3*H*-indoles to steric hindrance. Although one should be aware that the hydrogen atoms find themselves at calculated positions, the (non-bonded) distances between the azomethine nitrogen atoms N(1) and the *ortho* hydrogen atoms H(18), 2.47 in **1DA** and 2.49 Å in **2DA**, are significantly shorter than the sum of their contact radii, 2.75 Å (using contact radii of 1.20 for H and 1.55 Å for N). In **4DA** and **5DA** the corresponding distances are 2.63 and 2.59 Å, demonstrating that steric crowding is less severe. The distances between H(121) and H(81) in **1DA** and H(121) and H(91) in **2DA** are 2.12 and 2.13 Å, respectively, shorter than the sum of contact radii (2.40 Å) as well. The steric repulsion between these atoms has no counterpart in the benzylideneanilines and provides additional strain energy. Thus, fixation of the aniline rings X by a isopropylidene bridge forces these rings into a planar arrangement, but concomitantly the phenyl groups Y are more twisted out of the plane than the benzylideneanilines. The net result is that for **2DA** a gain and for **1DA** a loss in planarity is achieved in comparison to their related benzylideneanilines.

It is interesting to establish whether in the phenyl rings of the 3*H*-indoles a higher degree of quinoid character, reflecting a stronger ground state donor–acceptor interaction, is found than in those of the benzylideneanilines. The contribution of a quinoid resonance form in the ground state can be quantitively expressed by the parameter *Q*,[37] which for **1DA** and **2DA** is defined as eqn. (1) where *d* is the distance between the indicated

$$Q = 1/4(d_{1\text{–}2} + d_{3\text{–}4} + d_{4\text{–}5} + d_{1\text{–}6}) - 1/2(d_{2\text{–}3} + d_{5\text{–}6}) \text{ for ring X} \quad (1a)$$

$$Q = 1/4(d_{11\text{–}12} + d_{13\text{–}14} + d_{14\text{–}17} + d_{11\text{–}18}) - 1/2(d_{12\text{–}13} + d_{17\text{–}18}) \text{ for ring Y} \quad (1b)$$

carbon atoms (see Fig. 1). For benzylideneanilines **4DA** and **5DA** *Q* is given by the bond lengths between atoms at the same positions as in the 3*H*-indoles. The data in Table 5 demonstrate that in both rings X and Y *Q* is systematically larger for the 3*H*-indoles than for the analogously substituted benzylideneanilines. In the case of the aniline group X in **1DA** and **2DA** this is in line with the expectation that the smaller torsion angle leads to an increased donor–acceptor interaction. The large admixture of quinoid character in the benzylidene rings Y in both **1DA** and **2DA** is however surprising, as these rings are

Table 3 Crystal data and details of the structure determination of **1DA** and **2DA**

	1DA	**2DA**
Crystal data		
Formula	$C_{18}H_{19}N_3O_2$	$C_{18}H_{19}N_3O_2$
Molecular mass	309.37	309.37
Crystal system	Monoclinic	Monoclinic
Space group	$P2_1/c$ (No 14)	$P2_1$ (No 4)
a, *b*, *c*l Å	8.9238(6), 11.1106(10), 16.193(1)	8.209(2), 10.517(2), 9.130(2)
β/°	105.11(1)	105.67(2)
V/Å^3	1550.0(2)	759.0(3)
D_c/g cm^{-3}	1.326	1.3537(5)
Z	4	2
F(000)	656	328
μ/cm^{-1}	0.9	0.9
Crystal size/mm, colour	0.25 × 0.28 × 0.35, red	0.15 × 0.40 × 0.40, orange
Data collection		
T/*K*	150	150
θ_{min}, θ_{max}	1.30, 27.50	1.94, 27.50
Radiation	Mo-Kα, 0.710 73 Å	Mo-Kα, 0.710 73 Å
Δ*ω*/°	0.50 + 0.35 tan *θ*	0.96 + 0.35 tan *θ*
Horiz, vert aperture/mm	3.00, 4.00	3.56, 4.00
X-Ray exposure time/h	15	19
Linear decay (%)	4.0	5.2
Reference reflections	2 1 3, 3, 2 2, 3 $\bar{2}$ 2	$\bar{2}$ 1 4, $\bar{3}$ $\bar{1}$ 2, $\bar{2}$ 2 5
Data set	*h* −9:11; *k* 0:14; *l* −21:20	*h* −10:10; *k* −12:13; *l* −11:11
Total data	5758	6282
Total unique data	3562 (R_i = 0.0572)	3003 (R_i = 0.0888)
Observed data	3562	3003
Refinement		
No. of refl. params.	3562, 212	3003, 212
Weighting scheme (w^{-1})	$\sigma^2(F_o^2) + (0.0585P)^2 + 0.86P$	$\sigma^2(F_o^2) + (0.036P)^2$
Final R_1,[a] wR_2,[b] *S*	0.0574, 0.1567, 1.073	0.0448, 0.0987, 1.019
$(\Delta/\sigma)_{av}$ and max. in final cycle	0.000, 0.000	0.000, 0.000
Min. and max resd. dens/e A^{-3}	−0.33, 0.39	−0.19, 0.19

[a] $R_1 = \Sigma||F_o| - |F_c||/\Sigma|F_o|$. [b] $wR_2 = [\Sigma[w(F_o^2 - F_c^2)^2]/\Sigma(w(F_o^2)^2)]^{1/2}$.

Table 4 Selected bond lengths in **1DA** and **2DA**

Bond	**1DA**/Å	**2DA**/Å	Bond	**1DA**/Å	**2DA**/Å
O(1)–N(*x*) [a]	1.225(3)	1.225(3)	O(2)–N(*x*) [a]	1.232(3)	1.230(3)
N(1)–C(1)	1.403(3)	1.401(3)	N(1)–C(10)	1.293(3)	1.305(3)
N(2)–C(4)	1.373(3)	1.468(3)	N(*y*)–C(15) [b]	1.452(3)	1.448(4)
N(*y*)–C(16) [b]	1.445(3)	1.447(4)	N(3)–C(14)	1.465(3)	1.363(4)
C(1)–C(2)	1.386(4)	1.385(3)	C(1)–C(6)	1.390(4)	1.401(3)
C(2)–C(3)	1.381(3)	1.383(4)	C(3)–C(4)	1.413(4)	1.383(3)
C(4)–C(5)	1.413(4)	1.393(3)	C(5)–C(6)	1.381(3)	1.377(4)
C(6)–C(7)	1.517(3)	1.502(4)	C(7)–C(8)	1.540(3)	1.522(4)
C(7)–C(9)	1.529(4)	1.545(3)	C(7)–C(10)	1.536(3)	1.549(4)
C(10)–C(11)	1.479(3)	1.452(4)	C(11)–C(12)	1.393(4)	1.400(3)
C(11)–C(18)	1.409(3)	1.402(4)	C(12)–C(13)	1.388(3)	1.374(4)
C(13)–C(14)	1.382(3)	1.410(3)	C(14)–C(17)	1.377(4)	1.407(4)
C(17)–C(18)	1.373(3)	1.370(4)			

[a] N(*x*): N(3) in **1DA**, N(2) in **2DA**. [b] N(*y*): N(2) in **1DA**, N(3) in **2DA**.

more twisted in the 3*H*-indoles than in the benzylideneanilines. This unexpected finding may be tentatively explained by assuming that a planar arrangement of rings X is essential for a substantial quinoid contribution. The larger quinoid contributions in the 3*H*-indoles are also reflected by the lengths of the C=N bonds; these bonds are longer in **1DA** [1.293(3)] and **2DA** [1.305(3)] than in **4DA** [1.258(4)] and **5DA** [1.279(4) Å].

Another salient feature is that in both the dimethylaminophenyl and nitrophenyl group *Q* is larger for **2DA** than for **1DA** and larger for **5DA** than for **4DA**. This observation is fully in line with the finding that the orientation of the azomethine bridge in **4DA** and **1DA** obstructs the transmission of substituent effects towards the bridge, giving rise to a less pronounced donor–acceptor interaction.[19] The gain in quinoid character upon going from the benzylideneanilines to the 2-phenyl-3*H*-indoles is however larger for **1DA** than for **2DA**. This is possibly related to the fact that in **1DA** the 3*H*-indole moiety bears the dimethylamino group. The amount of quinoid character induced by the dimethylamino substituent is larger than that caused by the nitro substituent, indicating that the dimethylamino substituent effect is less strongly damped. In addition, it was seen above that the planar arrangement of the 3*H*-indole group is of particular interest for a favourable donor–acceptor interaction. It is invoked that it is the combination of these two factors that leads to the relatively large gain in quinoid character for **1DA**.

Table 5 Quinoid character of the benzene-type moieties in donor–acceptor substituted 3,3-dimethyl-2-phenyl-3*H*-indoles **1DA** and **2DA** and benzylideneanilines **4DA** and **5DA**

	Ring	*Q*/Å		Ring	*Q*/Å
1DA	X	0.020	**4DA**	X	0.013
1DA	Y	0.010	**4DA**	Y	0.005
2DA	X	0.011	**5DA**	X	0.007
2DA	Y	0.033	**5DA**	Y	0.027

3*H*-Indole **1DA** crystallizes in the monoclinic $P2_1/c$ space group. At first sight, the centrosymmetric nature of this space group renders the crystals unsuitable for macroscopic nonlinear optical phenomena.[13] However, in the solid state **1DA** possesses a chiral axis, since the phenyl group Y is rotated (18°) out of the 3*H*-indole plane. In the unit cell (Fig. 2), which contains four molecules, molecules are packed in two pairs, each pair consisting of an *R* and an *S* enantiomer. In its packing motif parallel alternating strands of the two enantiomeric forms are found. This alignment offers the interesting possibility of second-harmonic generation by use of circularly polarized light; the two enantiomers interact differently with circu-

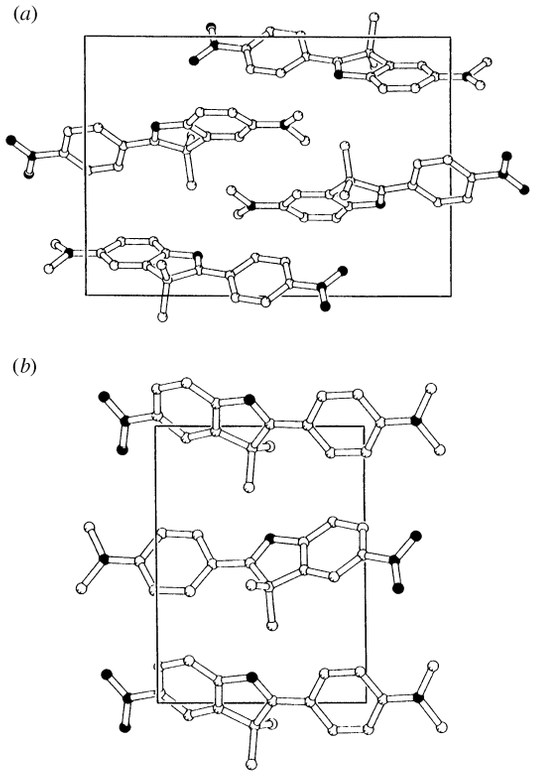

Fig. 2 Solid state packing of (*a*) **1DA** and (*b*) **2DA**. The view of the unit cell is along the *a* axis in (*a*) and along the *c* axis in (*b*). Hydrogen atoms are omitted for clarity.

larly polarized light, through which the centrosymmetry is distorted.[38,39]

Compound **2DA**, for which frozen-in chirality is observed as well, crystallizes in the monoclinic, chiral $P2_1$ group. In the unit cell, containing two molecules mutually related by a two-fold screw-axis, only one enantiomer is found (Fig. 2). It is however likely that single crystals consist of two types of domains, the first containing one enantiomer and the second the other enantiomer. Nevertheless, owing to the noncentrosymmetric order in principle a macroscopic NLO response can be anticipated from the crystals of **2DA**. The expected macroscopic nonlinear optical properties of **1DA** and **2DA** require further investigation.

Electronic properties

It is well established that electronic absorption spectra are known to be sensitive to the geometry of a π-system.[33] The transition energy *E* will increase upon twisting around an essential single bond (with a general torsion angle *a*), since resonance interactions between donor and acceptor orbitals are diminished. The loss in resonanace energy can be approximated to follow a $\cos^2 a$ dependence. A similar dependence on *a* has been derived, albeit empirically, for the extinction coefficient.[33] Consequently, the oscillator strength *f*, given by eqn. (2), where ε_{max}

$$f = 4.32 \times 10^{-9} \varepsilon_{max} \Delta\nu_{1/2} \qquad (2)$$

is the extinction coefficient at maximum absorption and $\Delta\nu_{1/2}$ the band width at half height, obeys the same law, provided that the band width is unaffected by rotation. The transition dipole moment μ_{ge}, to be obtained from eqn. (3), with $3he^2/8\pi^2 m_e =$

$$|\mu_{ge}|^2 = \frac{3he^2 f}{8\pi^2 m_e \omega_{max}} \qquad (3)$$

7.095×10^{-43} C^2 m^2 s^{-1} and ω_{max} the frequency at maximum absorption is then expected to be a more sensitive function of *a*, since ω_{max} also increases with *a*.

Characteristics of electronic absorption spectra of compounds **1–6d**, **1–6A** and **1–6DA** are compiled in Table 6. Those of the monosubstituted fluorenes and biphenyls nicely follow the rules outlined above. The transitions of the planar fluorenes occur at lower energies and are more intensive than the bands of the corresponding biphenyls. The increase in transition dipole moment of **3A** is however smaller than anticipated from the extinction coefficient, because the band width $\Delta\nu_{1/2}$ is rather small.

Comparison of the spectra of the 3*H*-indoles and benzylideneanilines (Fig. 3) is less straightforward. It has been pointed out that the electronic spectra of nitro-substituted benzylideneanilines **4A** and **5A** are complicated as a result of the nonplanar geometry of these compounds and the overlap of several transitions.[28,30] For **1A** and **2A** the overlap of bands is less pronounced and the most red shifted UV bands dominate their spectra. Our PPP/SCF/CI calculations[19] suggest that the corresponding transitions are of π–π* character (in line with CNDO/S calculations[30]), and are accompanied by predominant CT from the unsubstituted phenyl group to the nitro group. The position of the bands shifts slightly bathochromic upon moving from the benzylideneanilines to the 3*H*-indoles, while extinction coefficients ε_{max} increase significantly. The gain in transition dipole moment μ_{ge} is however less pronounced, since the bands of the 3*H*-indoles are substantially narrower. This narrowing of the band width is possibly caused by a smaller number of submerged bands; transitions based on interaction of the azomethine lone pair with the π-system are for instance not feasible in the 3*H*-indoles, since the lone pair lies in the nodal plane of the π-system. Another factor which may be responsible for the narrow band widths in the spectra of the 3*H*-indoles is the increased rigidity of these compounds (*vide infra*).

Electronic spectra of the donor benzylideneanilines **4D** and **5D** and the donor 3*H*-indoles **1D** and **2D** are in contrast to those of the similarly shaped nitro compounds and only small differences in maxima and intensities are encountered. Although bands can also be composed of several transitions, the resemblance between spectral characteristics indicates that geometries of benzylideneaniline and 3*H*-indole analogues are not very different. For **2D** and **5D** this can be rationalized by the fact that the dimethylaminophenyl moiety Y is free to rotate in both compounds. Nevertheless, the small bathochromic and hyperchromic effects present may be attributed to the coplanar orientation of the ring labelled X in **2D**.

The CT bands of the donor–acceptor substituted compounds **1DA**, **2DA** and **3DA** are shifted bathochromic with respect to those of their unfixed analogues. The shift for **1DA** is only small, while its extinction coefficient is smaller than that of **4DA**. Assuming that the steric repulsion that was found to distort the X-ray geometry of **1DA** is present in solution as well, it is likely that **1DA** will be the more twisted compound. However, since $\cos^2 a$ is a slowly varying function for small values of *a*, it may be insecure to treat the differences between the spectra of **1DA** and **4DA** in terms of torsion angles; other subtle factors may be of interest as well.§ In contrast, the distinct bathochromic shift on moving from **5DA** to **2DA** (1600 cm^{-1}) unambiguously reflects the large twist angle present in **5DA**.[28] A somewhat smaller, but still significant difference of 1100 cm^{-1} between the maxima of fluorene **3DA** and biphenyl **6DA** is found. Thus, it leaves little doubt that **6DA** is twisted in solution, although the PM3 calculations indicated that this compound is planar.

Remarkably, the intensities of the CT bands of the donor–

§ One of these factors is the presence of the isopropylidene bridge in the 3*H*-indoles. It is however supposed that the effect of a *meta* positioned isopropylidene group is negligible.

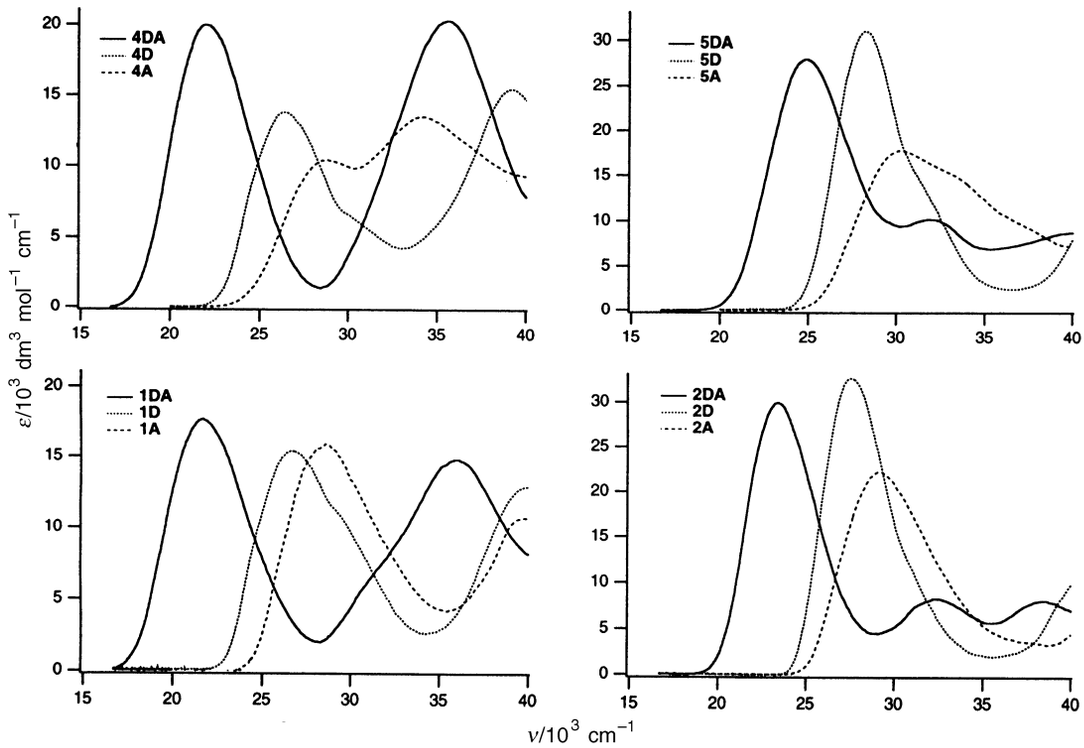

Fig. 3 UV–VIS spectra of bensylideneanilines (top) and 2-phenyl-3,3-dimethyl-3*H*-indoles (bottom) in chloroform

Table 6 Electronic absorption characteristics of compounds **1–6D**, **1–6A** and **1–6DA** in chloroform

	ν_{max}/10^3 cm^{-1}	ε_{max}/10^3 dm^3 mol^{-1} cm^{-1}	$\Delta\nu_{1/2}$ [a]	μ_{ge}/D [b]		ν_{max}/10^3 cm^{-1}	ε_{max}/10^3 dm^3 mol^{-1} cm^{-1}	$\Delta\nu_{1/2}$ [a]	μ_{ge}/D [b]
1D	26.7	15.4	4.75	5.01	**4D**	26.6	13.8	4.66	4.72
2D	27.5	32.7	3.70	6.35	**5D**	28.3	31.0	4.00	6.34
3D	32.3	24.1	5.15	5.93	**6D**	33.2	19.1	4.66	4.96
1A	28.5	15.9	5.06	5.09	**4A**	28.8	10.4	6.23	4.54
2A	29.2	22.2	4.68	5.71	**5A**	30.2	17.8	5.56	5.48
3A	29.8	18.3	4.53	5.06	**6A**	32.4	16.0	5.46	4.97
1DA	21.6	17.7	3.93	5.72	**4DA**	22.0	19.9	4.56	6.10
2DA	23.3	30.0	3.74	6.65	**5DA**	24.9	28.2	4.72	7.00
3DA	23.4	22.2	4.48	6.24	**6DA**	24.5	23.0	4.82	6.45

[a] Band width at half height in units of 10^3 cm^{-1}. [b] 1 D = 3.336 × 10^{-30} C m.

acceptor compounds, as measured by the transition dipole moments μ_{ge}, decrease upon fixation. Although the extinction coefficients of **1DA** and **3DA** are already smaller than those of **4DA** and **6DA**, respectively, the main source of the decrease in transition moment are the narrow band widths $\Delta\nu_{1/2}$, which are caused by the increased rigidity of the fixed compounds. The rigidity results in relatively steep potential energy curves for both the ground and excited states. Consequently, a (Franck–Condon) transition is allowed for a smaller number of vibrational states, which leads to a smaller band width. This effect is particularly prominent for the donor–acceptor compounds, since intramolecular CT bands are usually very broad as a result of substantially differing ground and excited state geometries. As was seen above peaks of the nitro-substituted 3*H*-indoles **1A** and **2A** and fluorene **3A** are also much narrower than those of the respective benzylideneanilines **4A** and **5A** and biphenyl **6A**, which may however be partly caused by the smaller number of overlapping bands. In the dimethylamino compounds the effect is not clearly observable.

Redox potentials of related 3*H*-indoles and benzylideneanilines are hardly different (Table 7). Hence, they prove not to be sensitive to the molecular geometry. With respect to the donor oxidation potentials this observation is in agreement with the limited variance of the PM3 calculated ionization potentials with torsion. Neither the conformation nor the electron lone pair on the azomethine nitrogen atom appears to have a significant effect on the redox potentials. In common with benzylideneanilines, stilbenes and azobenzenes[19] oxidation potentials of the donor–acceptor 3*H*-indoles are somewhat more positive and reduction potentials are somewhat more negative than the potentials of the respective monosubstituted compounds, which is to be attributed to the occurrence of ground state interactions. In the fluorene and biphenyl series there is a more distinct difference between the oxidation potentials of both **3D** and **6D** and **3DA** and **6DA** than found for the 3*H*-indoles. The lower oxidation potentials of

Table 7 First oxidation and reduction potentials of compound series **1–6D, 1–6A** and **1–6DA**

	E_{ox}/eV	E_{red}/eV		E_{ox}/eV	E_{red}/eV
1D	+0.52	−2.21	**4D**	+0.58	*a*
2D	+0.74	−2.31	**5D**	+0.76	*a*
3D	+0.51	*a*	**6D**	+0.64	*a*
1A	+1.77	−1.07	**4A**	+1.76	−1.08
2A	+1.92	−1.19	**5A**	+1.88	−1.20
3A	+1.90	−1.24	**6DA**	*a*	−1.21
1DA	+0.58	−1.10	**4DA**	+0.63	−1.10
2DA	+0.81	−1.26	**5DA**	+0.85	−1.23
3DA	+0.66	−1.30	**6DA**	+0.75	−1.26

[a] Not observed.

Table 8 Fluorescence solvatochromism and two-level hyperpolarizabilities $\beta_{CT}(0)$ of donor–acceptor substituted compounds

		1DA		**2DA**		**3DA**		**6DA**	
Solvent	Δf	$\nu_{abs}/10^3$ cm^{-1}	$\nu_{fl}/10^3$ cm^{-1}	$\nu_{abs}/10^3$ cm^{-1}	$\nu_{fl}/10^3$ cm^{-1}	$\nu_{abs}/10^3$ cm^{-1}	$\nu_{fl}/10^3$ cm^{-1}	$\nu_{abs}/10^3$ cm^{-1}	$\nu_{fl}/10^3$ cm^{-1}
Cyclohexane	−0.002	22.3	18.8	24.5	21.0	25.1	21.4	26.6	21.6
Dibutyl ether	0.096	22.4	17.0	24.2	19.5	24.7	19.4	25.8	19.5
Diethyl ether	0.162	22.6	15.8	24.2	18.9	24.5	17.9	25.7	18.1
Ethyl acetate	0.200	22.2	14.0	23.8	17.1	24.0	16.5	25.2	16.0
THF	0.210	21.9	14.0	23.6	17.2	23.9	16.5	24.7	16.1
Acetonitrile	0.305		*a*	23.5	13.7	23.6	14.0	24.7	13.7
$C/10^3$ cm^{-1}		3.48		2.87		3.62		4.69	
$(2\Delta\mu^2/hc\rho^3)/10^3$ cm^{-1}		21.49		19.73		18.89		20.21	
r [b]		0.992		0.951		0.996		0.985	
$\Delta\mu$/D		16.8		16.1		14.9		15.4	
$\beta_{CT}(0)/10^{-30}$ esu		30		33		27		27	

[a] No fluorescence observed. [b] Correlation coefficient.

the fluorenes reflect the increased interaction of the dimethylamino group with the planar π-systems. Reduction potentials of the fluorenes and biphenyls are of similar magnitude.

Despite the occurrence of changes in electronic spectra when going from the benzylideneanilines to the 3*H*-indoles, mostly related to the presence of other geometries, differences as a result of the orientation of the azomethine bridge are maintained. Series **1** and **4** absorb at lower energies than series **2** and **5**, while the absorptions of the latter series are more intense. It has been shown[19] that the electronic spectra of the benzylideneanilines are strongly related to their redox potentials, which, in turn, are predominantly determined by the position of the nitrogen atom in the bridge. In the benzylideneanilines of type **4**, the electronegative azomethine nitrogen atom raises the oxidation potential of the dimethylamino donor, while the electropositive carbon atom lowers the reduction potential. This results in a smaller HOMO–LUMO gap and hence a smaller excitation energy, but concomitantly the transition dipole moment is lowered. The same appears to be true for the 3*H*-indoles. It is thus shown that the observed electronic spectral diferences between the two types of benzylideneanilines are of electronic rather than of conformational origin.

Nonlinear optical properties

Following the two-level model as elaborated in the preceding paper[19] the effects of conformational locking on the electronic transitions are presumed to express themselves in $\beta_{CT}(0)$ of the donor–acceptor compounds. Transition dipole moments and energies are already listed in Table 6. Fluorescence date and solvatochromic plot parameters for **1DA**, **2DA**, **3DA** and **6DA** are collected in Table 8. Previously obtained solvatochromic sensitivities ($2\Delta\mu^2/hc\rho^3$) and $\Delta\mu$ values (differences in excited and ground state dipole moments) for benzylideneanilines are 21 450 cm^{-1} and 16.8 D for **4DA** and 17 800 cm^{-1} and 15.3 D for **5DA**.[19] The effective radius used for 3*H*-indoles **1DA** and **2DA** was 5.1 Å *i.e.* the same radius as used for the benzylideneaniline derivatives. For the biphenyl **6DA** (length 14.5, diameter 6.5 Å, as measured from a CPK model) and fluorene **3DA** an effective radius of 4.9 Å was applied.

The $\Delta\mu$ values show that fixation of the geometry has only a limited effect; comparable values are found for analogously substituted benzylideneanilines and 3*H*-indoles and for **6DA** and **3DA**. It may however be argued that effective radii for the planar-locked species should be larger than those of the unlocked species and that therefore their $\Delta\mu$ values are underestimated. Correction for the radii however results in only a small to moderate increment in $\Delta\mu$. Applying $\rho = 5.3$ Å, $\Delta\mu$ values of 17.8 D (**1DA**) and 17.1 (**2DA**) are obtained.

The $\Delta\mu$ values of the benzylideneanilines are somewhat smaller than those of the 3*H*-indoles, which is in contrast to what is expected; for $\Delta\mu$ an increase upon rotation is expected, as donor and acceptor orbitals are more strongly decoupled and separated charges are more localized on the respective chromophores. Although as a result of the approximations involved a definite conclusion is thus difficult to draw, the presence of an additional saturated bridge does not strongly influence $\Delta\mu$ data, and hence the degree of charge transfer. This is supported by the fact that differences in solvatochromic sensitivities are small as well.

The two-level hyperpolarizabilities obtained, $\beta_{CT}(0)$, are included in Table 8. The $\beta_{CT}(0)$ values of **4DA** and **5DA** are 33×10^{-30} and 31×10^{-30} esu, respectively.[19] It is seen that $\beta_{CT}(0)$ values for the 3*H*-indoles and the fluorene are of similar magnitude as those found for the respective benzylideneanilines and biphenyl. This is not in line with expectation since the PM3 calculations have suggested that a decrease of θ and φ should lead to a larger hyperpolarizability, although **4DA** may be more planar that **1DA**. The reason that the $\beta_{CT}(0)$ value of the 3*H*-indoles and the fluorene does not come up to expectations is connected to their small transition dipole moments. It was shown above that these transition dipole moments are relatively small because of narrow band widths. Following the two-level model the smaller transition dipole moments counterbalance the favourable red shifts of the electronic transitions in the case of **2DA** and **3DA**. As **1DA** and **4DA** have comparable transition energies, the decrease in μ_{ge} results in a lower $\beta_{CT}(0)$ for **1DA**.

First hyperpolarizabilities determined with the EFISH technique[40–42] are compiled in Table 9. Dipole moments of planar-locked compounds, required in order to extract $\beta(0)$ from the experimentally measured $\mu_g\beta$ data,¶ were assessed as equal to those of their non-planar analogues, which were taken from the literature.[43,44] The PM3 calculated ground state dipole moments, μ_{calc}, given in Table 1 show that this is not a gross oversimplification. In the twist angles ranges in which **4DA**–**6DA** preferentially occur ($\theta \approx 0$–$30°$ and $\varphi \approx 0$–$30°$ for **4DA**, $\theta \approx 0$–$90°$ and $\varphi \approx 0$–$30°$ for **5DA** and $\theta \approx 0$–$60°$ for **6DA**) μ_{calc} values do not change very significantly. Nevertheless, in view of the uncertainty in dipole moments it may also be of interest to evaluate $\mu_g\beta(0)$ data. They however reveal the same features as the $\beta(0)$ values described below.

The EFISH $\beta(0)$ data demonstrate that for the monosubstituted compounds a small to moderate gain is achieved upon fixing the conformation. The only exception is $\beta(0)$ of **2A**, which is slightly smaller than that of **5A**. A possible explanation is that

¶ In contrast to data described in the preceding paper,[19] hyperpolarizabilities of **1D**, **2D**, **4D** and **5D** were not corrected for the angles of *ca.* 40° between the dipole moment and hyperpolarizability vectors. PM3 calculations indicate that planarization does not affect these angles significantly.

Table 9 EFISH first hyperpolarizabilities of compounds **1–6D, 1–6A** and **1–6DA**

	μ_g/D	$\mu_g\beta/10^{-48}$ esu	$\mu_g\beta(0)/10^{-48}$ esu	$\beta(0)/10^{-30}$ esu		μ_g/D	$\mu_g\beta/10^{-48}$ esu	$\mu_g\beta(0)/10^{-48}$ esu	$\beta(0)/10^{-30}$ esu
1D	2.7	28.1	22.8	8.4	**4D**	2.7	21.6	17.6	6.5
2D	3.6	69.7	57.6	16	**5D**	3.6	46.6	38.8	11
3D	2.0	18.6	16.1	8.1	**6D**	2.0	18.6	15.7	7.9
1A	4.2	45.7	38.1	9.1	**4A**	4.2	37.4	31.4	7.5
2A	5.0	39.8	33.5	6.7	**5A**	5.0	42.7	36.5	7.3
3A	4.3	41.8	35.4	8.2	**6A**	4.3	29.2	25.4	5.9
1DA	6.9	443.1	318.8	46	**4DA**	6.9	416.7	304.2	44
2DA	8.6	400.3	300.9	35	**5DA**	8.6	390.1	304.8	35
3DA	6.8	310.6	235.3	35	**6DA**	6.8	305.2	236.6	35

[a] Ground state dipole moments of unfixed compounds were taken from McClennan[43] and were measured in benzene at 25 °C; for all benzylideneanilines the temperature was not specified.[44]

in planar **2A** the CT interaction between the azomethine lone pair and the nitro group, which should be connected with a substantial contribution to β, is not possible. Invoking the validity of the two-level model for evaluation of the hyperpolarizabilities of the monosubstituted compounds it is seen that the increase $\beta(0)$ is either caused by a red shift of the electronic transition (**2D**, **3A**), an increase of the transition dipole moment (**1D**, **1A**) or a combination of both (**3D**).

The EFISH hyperpolarizabilities of the donor–acceptor substituted 3*H*-indoles and fluorene equal those of their unfixed analogues. Evidently, fixation of the benzylideneanilines and biphenyls in a planar conformation does not lead to an increase of β. Since the absence of a torsion effect was already noted for the two-level hyperpolarizabilities, it is readily understood that the absence of a gain in $\beta(0)$ upon fixation is caused by the concomitant effects of a bathochromic shift and a decrease in intensity of the CT transition. Note however that the EFISH hyperpolarizabilities of **2DA** and **3DA** are in line with the two-level hyperpolarizabilities, while the EFISH hyperpolarizability of **1DA** is substantially larger than the two-level value.

The NLO properties of biphenyl and fluorene derivatives have been discussed before by Cheng *et al.*[6] They reported hyperpolarizabilities of 55×10^{-30} and 50×10^{-30} esu for **3DA** and **6DA**, respectively (in chloroform), data which are uncorrected for dispersion (fundamental wavelength 1.91 μm). Furthermore other ground state dipole moments were used. Correction for dispersion and applying the present dipole moment gives hyperpolarizabilities of 37×10^{-30} (**3DA**) and 32×10^{-30} esu (**6DA**), of a magnitude comparable to our data and with a mutual difference that can be considered small. Cheng *et al*. evaluated the difference in terms of the excitation energy and the extinction coefficient of the CT band. The present study shows that besides the excitation energy the transition dipole moment rather than the extinction coefficient is of particular interest.

Conclusions

Although PM3 calculations indicate that a small to moderate increase in hyperpolarizability can be achieved by locking the benzylideneaniline and biphenyl conjugation paths in a planar conformation it is experimentally demonstrated that the actual gain is either small or negligible. In particular hyperpolarizabilities of donor–acceptor substituted compounds, which exhibit the largest and most useful nonlinear optical properties, are of equal magnitude for conformationally locked and unlocked analogues. The reason that the hyperpolarizabilities of the planar-locked compounds lag behind expectations is that their relatively small transition dipole moments counterbalance the effect of bathochromic shifts. The decrease in transition dipole moment is caused by narrower band widths, a consequence of the increased rigidity of the planar-locked molecules. Hence, it is concluded that fixing the benzylideneaniline and biphenyl conjugation paths (and probably π-conjugation paths in general) in a planar conformation by a chemical method, *i.e.* by use of a saturated bridge, is ineffective in increasing β.‖ Moreover, the X-ray structure of **1DA** shows that the presence of such a bridge does not necessarily lead to a more planar structure.

The hyperpolarizabilities of the benzylideneaniline **4DA** and 3*H*-indole **1DA**, where the azomethine nitrogen atom is linked to the dimethylaminophenyl group are larger than those of **2DA** and **5DA**. Since the molecular geometry does not affect the hyperpolarizabilities of benzylideneanilines **4DA** and **5DA** the difference between them is of electronic rather than of conformational origin. The explanation[25] that the non-planar structure of **5DA** is responsible for its smaller hyperpolarizability is thus not correct.

Since trends in hyperpolarizabilities and electronic transition characteristics of 3*H*-indoles are essentially identical to those of analogous benzylideneanilines, the conclusions drawn in the preceding paper[19] remain valid. Thus, differences in nonlinear optical activities of monosubstituted benzylideneanilines are mainly based on the transition dipole moment μ_{ge}, while the larger $\beta(0)$ of **4DA** in comparison to **5DA** reflects an interplay between CT transition intensities and energies.

Experimental

General

^{1}H (300 MHz) and ^{13}C NMR (75 MHz) spectra were recorded on a Bruker AC 300 spectrometer and are referenced to external Me_4Si. IR spectra were recorded for powdered dispersion in KBr in diffuse reflectance mode with a Mattson Galaxy Series FTIR 5000 spectrometer. Melting points were determined on a Mettler FP5/FP51 photoelectric apparatus. Cyclic voltammetry measurements were performed using an EG&G Model 273 or a Heka PG 287 potentiostat/galvanostat at a scan rate of 0.1 V s^{-1}. Solutions of 0.5 g l^{-1} in acetonitrile (Janssen p.A. grade, dried on 3 Å molecular sieves or by distillation from calcium hydride) were used, 0.1 M tetrabutylammonium hexafluorophosphate (Fluka, electrochemical grade) being present as supporting electrolyte. Redox potentials were measured relative to $Ag/AgNO_3$ (0.01 M) and were converted into values relative to standard calomel electrode (SCE) by measuring the oxidation potential of the $FeCp/FeCp^{\bullet+}$ (Cp = cyclopentadienyl) couple ($E_{1/2}$ *vs.* SCE = 0.31 V[45]). The equipment and procedures used for optical and photophysical measurements have been described previously.[19]

Details of PM3 calculations have been described elsewhere.[19] Geometry optimizations of rotational conformers were carried out by fixing dihedral angles θ and φ at the indicated magnitudes (Table 2) and allowing a full optimization of all other coordinates. Calculations on **4DA** and **5DA** were performed on

‖ The PM3 calculations show, however, that it is likely that planarity of a given π-system (which is not chemically fixed) results in an optimal nonlinear optical activity.

dimethylamino-nitro-substituted 2-phenyl-3*H*-indoles as model compounds (MOPAC version 6.0).[46]

Crystal structure determination and refinement of 1DA and 2DA

Crystals suitable for X-ray diffraction were obtained by slow evaporation of a solution of **2DA** in ethyl acetate–hexane (1:4 v/v) and by crystallization of **1DA** from ethyl acetate. Crystals of both compounds were glued to glass fibres and transferred to an Enraf-Nonius CAD-4T (rotating anode, graphite monochromated Mo-Kα radiation) diffractometer for data collection at 150 K. Unit cell parameters were determined from a least-squares treatment of the SET4 setting angles of 25 reflections and were checked for the presence of higher lattice symmetry.[47] All data were collected in $\omega/2\theta$ scan mode, data were corrected for Lorentz polarization and for the observed linear decay of the intensity control reflections. Redundant data were merged into a unique data set. The structures were solved with direct methods (SHELXS86[48]) followed by subsequent difference Fourier syntheses. Refinement on F^2 with all unique reflections was carried out by full-matrix least-squares techniques. Hydrogen atoms were introduced on calculated positions and included in the refinement riding on their carrier atoms with isotropic thermal parameters related to the U_{eq} of the carrier atoms. All non-hydrogen atoms were refined with anisotropic thermal parameters. Weights were introduced in the final refinement cycles. The absolute structure of **2DA** could not be determined unambiguously.

Crystal data and numerical details of the structure determinations are given in Table 3. Selected bond distances are listed in Table 4. Atomic coordinates, bond lengths and angles, and thermal parameters have been deposited at the Cambridge Crystallographic Data Centre (CCDC). For details of the deposition scheme, see 'Instructions for Authors', *J. Chem. Soc., Perkin Trans. 2*, 1997, Issue 1. Any request to the CCDC for this material should quote the full literature citation and the reference number 188/54. Neutral atom scattering factors and anomalous dispersion factors were taken from the International Tables for Crystallography.[49] All calculations were performed with SHELXL93[50] and the PLATON[51] package (geometrical calculations and illustrations) on a DEC-5000 cluster.

Syntheses

3*H*-Indoles were synthesized according to modified literature procedures[28] (*vide infra*). 2-(*N*,*N*-Dimethylamino)-7-nitrofluorene (**3DA**) was obtained by methylation of 2-amino-7-nitrofluorene.[52] 2-(*N*,*N*-Dimethylamino)fluorene (**3D**), 2-nitrofluorene (**3A**) and 4-nitrobiphenyl (**6A**) were purchased from Aldrich and were purified by recrystallization from ethanol. 4-(*N*,*N*-Dimethylamino)biphenyl (**6D**) was prepared *via* methylation of 4-aminobiphenyl following the procedure for **1D** described below. 4-(*N*,*N*-Dimethylamino)-4′-nitrobiphenyl (**6DA**) was prepared according to the literature.[53] Benzylideneanilines **4DA**, **4D**, **4A**, **5DA**, **5D** and **5A** were obtained from condensation of appropriately substituted benzaldehydes and anilines.[19,54] The purity of all compounds was established by thin layer chromatography, ^{1}H and ^{13}C NMR spectroscopy and infrared spectroscopy.

Syntheses of 3*H*-indoles were carried out in a nitrogen atmosphere. Ethanol used in preparations was dried by storing on 4 Å molecular sieves or by distillation from Mg/I_2.[55] Toluene was freshly distilled from sodium–benzophenone; dimethylformamide (DMF) was dried by storing on 3 Å molecular sieves. Column chromatography was performed on Merck Kieselgel 60 silica (230–400 ASTM).

3,3-Dimethyl-2-[4-(*N*,*N*-dimethylamino)phenyl]-5-nitro-3*H*-indole 2DA. A mixture of 4-nitrophenylhydrazine (1.64 g, 10.7 mmol) and 1-[4-(*N*,*N*-dimethylamino)phenyl]-2-methylpropan-1-one[56] (1.99 g, 10.4 mmol) was stirred at 110 °C for 3 h. Subsequently ethanol (20 ml) and ethanolic hydrogen chloride (40 ml) were added, upon which the mixture was heated at reflux for 80 min. After removal of volatiles under reduced pressure ice–water (100 ml) was added and the suspension was made alkaline by addition of 2 M aqueous sodium hydroxide. The aqueous mixture was extracted with methylene chloride (100 ml) and diethyl ether (4 × 100 ml). Thereafter the combined organic layers were dried over magnesium sulfate, filtered and concentrated under reduced pressure. The crude product was purified by column chromatography (eluent chloroform) followed by recrystallization from methanol. Yield 0.23 g (7%) of a red crystalline solid; mp 177 °C; ν_{max}(KBr)/cm^{-1} 3060, 2970 (Me), 2914 (Me), 2818 (NMe_2), 1607 (Ar C=C), 1510 (NO_2), 1450, 1366 (Me), 1325 (NO_2), 902 (Ar-H) and 818 (AR-H); δ_H($CDCl_3$) 8.26 (1 H, dd, Ar-H), 8.15 (1 H, d, Ar-H), 8.13 (2 H, AA′XX′, Ar-H), 6.76 (2 H, AA′XX′, Ar-H), 7.63 (1 H, d, Ar-H), 3.10 (6 H, s, NMe) and 1.64 (6 H, s, CMe); δ_C($CDCl_3$) 188.1 (C=N), 159.6, 152.6, 148.3, 144.8, 130.6, 124.8, 119.6, 119.5, 116.7, 111.4, 53.3 (*C*Me), 40.0 (NMe) and 25.2 (C*Me*).

3,3-Dimethyl-2-[4-(*N*,*N*-dimethylamino)phenyl]-3*H*-indole 2D.[56] A mixture of phenylhydrazine (0.92 g, 8.5 mmol) and 1-[4-(*N*,*N*-dimethylamino)phenyl]-2-methylpropan-1-one[56] (1.50 g, 7.8 mmol) was stirred at 110 °C for 3 h. Acetic acid (10 ml) was added and the mixture was refluxed for 75 min. After removal of the acetic acid by rotary evaporation and addition of 30 ml of 2.5 M aqueous sodium hydroxide the mixture was extracted with diethyl ether (3 × 50 ml). The combined extracts were dried on magnesium sulfate, filtered and evaporated. Purification by sublimation (70 °C at 0.01 mmHg) and recrystallization from ethanol–water (8:1 v/v) afforded **2D** (0.60 g, 29%) as a yellow crystalline solid; mp 118 °C; ν_{max}(KBr)/cm^{-1} 3044, 2969 (Me), 2936 (Me), 2812 (NMe_2), 1615 (Ar C=C), 1505 (Ar C=C), 1454, 1368 (Me), 824 (Ar-H) and 754 (Ar-H); δ_H($CDCl_3$) 8.11 (2 H, AA′XX′, Ar-H), 6.76 (2 H, AA′XX′, Ar-H), 7.62 (1 H, d, Ar-H), 7.32 (3 H, m, Ar-H), 7.20 (1 H, t, Ar-H), 3.07 (6 H, s, NMe) and 1.60 (6 H, s, CMe); δ_C($CDCl_3$) 183.3 (C=N), 154.0, 152.1, 147.8, 130.3, 127.8, 124.9, 121.0, 120.2, 111.7, 53.2 (*C*Me), 40.4 (NMe) and 25.6 (C*Me*).

3,3-Dimethyl-5-nitro-2-phenyl-3*H*-indole 2A. A solution of 4-nitrophenylhydrazine (8.5 g, 56 mmol) and 2-methyl-1-phenylpropan-1-one (8.5 g, 57 mmol) in toluene (175 ml) was heated at reflux in a flask equipped with a Dean–Stark water separator. After 20 h the toluene was removed under reduced pressure and ethanol (20 ml) and 20 ml of a 5–6 M solution of hydrogen chloride in isopropyl alcohol were added. The mixture was refluxed for 18 h, cooled to room temp., filtered and evaporated to dryness. The residue was taken up in ice–water and made alkaline by addition of 25 ml of 2 M aqueous potassium hydroxide. Crude **2A** was isolated after extraction with diethyl ether, drying (magnesium sulfate) and removal of the solvent in a rotary evaporator. The product was purified by column chromatography (eluent chloroform) and recrystallizations from ethanol and ethyl acetate–hexane 1:4 v/v. Yield 1.37 g (9%) of yellow crystals; mp 147 °C; ν_{max}(KBr)/cm^{-1} 3067, 2990 (Me), 2928 (Me), 1595 (Ar C=C), 1518 (NO_2), 1491 (Ar C=C), 1460, 1393, 1337 (NO_2), 887 (Ar-H), 833 (Ar-H), 735 (Ar-H) and 795 (Ar-H); δ_H($CDCl_3$) 8.29 (1 H, dd, Ar-H), 8.22–8.18 (2 H + 1 H, m + d, Ar-H), 7.75 (1 H, d, Ar-H), 7.55 (3 H, m, Ar-H) and 1.66 (6 H, s, CMe); δ_C($CDCl_3$) 188.2 (C=N), 158.3, 148.7, 145.9, 132.3, 131.8, 128.9, 128.9, 124.6, 120.9, 116.9, 54.2 (*C*Me) and 24.5 (C*Me*).

3,3-Dimethyl-5-(*N*,*N*-dimethylamino)-2-phenyl-3*H*-indole 1D. A mixture of 5-amino-3,3-dimethyl-2-phenyl-3*H*-indole[28] (1.19 g, 5.0 mmol), methyl iodide (1.5 ml, 24 mmol) and potassium carbonate (2.00 g, 14 mmol) in ethanol (25 ml) was heated at reflux for 18 h. After cooling to room temp. the mixture was filtered and the residue was washed with ice-cold ethanol (10 ml) and with water (2 × 10 ml). The resulting quaternary ammonium salt (1.08 g) was subsequently refluxed in ethanol-

amine for 1.5 h.[57] After addition of water the suspension was extracted with diethyl ether (4 × 50 ml). The combined organic layers were dried on magnesium sulfate and concentracted *in vacuo*. Recrystallization from hexane gave **1D** (0.50 g, 38%) as orange crystals; mp 117 °C; ν_{max}(KBr)/cm^{-1} 3045, 2974 (Me), 2926 (Me), 2808 (NMe_2), 1614 (Ar C=C), 1512 (Ar C=C), 1438, 1362 (Me), 843 (Ar-H), 796 (Ar-H), 774 (Ar-H) and 756 (Ar-H); δ_H[$(CD_3)_2SO$] 8.11 (2 H, m, Ar-H), 7.47 (3 H, m, Ar-H), 7.41 (1 H, d, Ar-H), 6.89 (1 H, d, Ar-H), 6.66 (1 H, d, Ar-H), 2.96 (6 H, s, NMe) and 1.51 (6 H, s, CMe); δ_C[$(CD_3)_2SO$] 180.1 (C=N), 151.9, 150.9, 145.6, 135.6, 132.1, 131.0, 129.9, 123.0, 113.7, 108.1, 55.0 (*C*Me), 43.1 (NMe) and 27.1 (C*Me*).

3,3-Dimethyl-2-(4-nitrophenyl)-3*H*-indole 1A. A solution of 2-methyl-1-(4-nitrophenyl)propan-1-one[28] (2.83 g, 14.6 mmol) and phenylhydrazine (1.60 g, 14.8 mmol) in toluene (75 ml) was heated at reflux overnight, during which water was separated with a Dean–Stark apparatus. The toluene was distilled off at reduced pressure and ethanol (15 ml) and 15 ml of a 5–6 M solution of hydrogen chloride in isopropyl alcohol were added. After boiling for 1 h a yellow precipitate was filtered off and washed with water and 2 M aqueous sodium hydroxide. 3*H*-indole **1A** was isolated by Soxhlet extraction with diethyl ether and was purified by recrystallization from ethanol followed by column chromatography (eluent chloroform). Yield 1.43 g (37%) of an orange solid; mp 144 °C. ν_{max}(KBr)/cm^{-1} 3080, 2978 (Me), 2935 (Me), 1593 (Ar C=C), 1524 (NO_2), 1493 (Ar C=C), 1452, 1346 (NO_2), 860 (Ar-H) and 752 (Ar-H), δ_H($CDCl_3$) 8.33 (4 H, AA′BB′, Ar-H), 7.74 (1 H, d, Ar-H), 7.38 (3 H, m, Ar-H) and 1.61 (6 H, s, CMe); δ_C[$(CD_3)_2SO$] 183.1 (C=N), 154.6, 150.8, 150.4, 140.6, 131.8, 130.4, 129.2, 126.8, 124.1, 123.6, 55.7 (*C*Me) and 26.1 (C*Me*).

4-(Acetylamino)phenylhydrazine hydrochloride.[58–60] At 0 °C, a solution of sodium nitrite (28.98 g, 420 mmol) in water (120 ml) was added dropwise to a solution of 4-aminoacetanilide (60.02 g, 400 mmol) in 240 ml of 6 M aqueous hydrochloric acid. After addition of diethyl ether (40 ml) a solution of tin(II) chloride dihydrate (240.48 g, 1.07 mol) in 340 ml of 12 M aqueous hydrochloric acid was added slowly to the cooled (0–10 °C) solution. When the addition was completed the suspension was stirred for another 30 min at 0 °C and filtered, leaving 72.78 g of a brown solid.

Subsequently 20 g of this solid was dissolved in 120 ml of boiling water and after cooling to 40 °C, stirred in a hydrogen sulfide atmosphere (balloon). After hydrogen sulfide consumption had ceased the mixture was cooled to 0 °C and filtered. Concentrated hydrochloric acid (120 ml) was added to the filtrate upon which a white solid precipitated. The precipitate was filtered off, washed with cold 6 M hydrochloric acid and dried in a vacuum desiccator. Unlike the procedure described in literature[59] the product was not purified by boiling in ethanol, since this step yielded 1,4-phenylenediamine as final product. Yield 5.79 g; δ_H(D_2O) 7.39 (2 H, AA′XX′, Ar-H), 7.06 (2 H, AA′XX′, Ar-H) and 2.15 (3 H, s, COMe).

5-Amino-3,3-dimethyl-2-(4-nitrophenyl)-3*H*-indole. In a one-necked flask solutions of 2-methyl-1-(4-nitrophenyl)propan-1-one[28] (4.57 g, 23.7 mmol) in ethanol (400 ml), 4-acetylaminophenylhydrazine hydrochloride (6.53 g, 32.4 mmol) in water (110 ml) and sodium acetate (4.70 g, 57.3 mmol) in water (10 ml) were mixed. After stirring at 60 °C for 18 h an orange precipitate had formed that was collected by filtration. The filtrate was stirred at 60 °C for another 17 h, after which another crop of orange solid was filtered off. The combined residues (1.94 g) were dried under reduced pressure and subsequently dissolved in a mixture of ethanol (40 ml) and 25 ml of 5–6 M hydrogen chloride in isopropyl alcohol. The solution was heated at reflux for 1 h, after which the solvents were removed using a rotary evaporator. Ice–water (100 ml) and 2 M sodium hydroxide were added to the residue, and the aqueous system was extracted with methylene chloride (3 × 50 ml). After drying on magnesium sulfate and evaporation of the solvent the resulting 5-amino-3*H*-indole was purified by column chromatography (eluent ethyl acetate), yielding 1.55 g (23%) of an orange solid; δ_H($CDCl_3$) 8.27 (4 H, AA′BB′, Ar-H), 7.52 (1 H, d, Ar-H), 6.70–6.66 (2 H, m, Ar-H), 4.1 (2 H, br, NH_2) and 1.56 (6 H, s, CMe).

5-(*N*,*N*-Dimethylamino)-3,3-dimethyl-2-(4-nitrophenyl)-3*H*-indole 1DA. A mixture of 5-amino-3,3-dimethyl-2-(4-nitrophenyl)-3*H*-indole (0.5 g, 1.7 mmol), potassium carbonate (0.55 g, 4.0 mmol), methyl iodide (5 ml, 80 mmol) and trimethyl phosphate (15 ml, 128 mmol) was stirred at 104 °C.[52] After 3 h the mixture was cooled with an ice-bath and 25 ml of 25% aqueous ammonia was added. The resulting solid was filtered off, washed with 6.5% aqueous potassium carbonate solution and subsequently dissolved in 100 ml of boiling DMF. After addition of water (100 ml) crude **2DA** was isolated by extraction with chloroform, drying on magnesium sulfate and evaporation of the solvent. Pure **2DA** (0.11 g, 21%) was obtained in the form of red–violet crystals after recrystallization from ethyl acetate; mp 214 °C; ν_{max}(KBr)/cm^{-1} 3086, 2960 (Me), 2924 (Me), 2810 (NMe_2), 1589 (Ar C=C), 1518 (NO_2), 1503 (Ar C=C), 1358 (Me), 1339 (NO_2), 856 (Ar-H) and 806 (Ar-H); δ_H($CDCl_3$) 8.28 (4 H, AA′BB′, Ar-H), 7.60 (1 H, d, Ar-H), 6.75–6.69 (2 H, m, Ar-H), 3.06 (6 H, s, NMe) and 1.59 (6 H, s, CMe); δ_C($CDCl_3$) 176.0 (C=N), 150.2, 149.7, 147.9, 143.4, 139.5, 128.2, 123.7, 122.2, 111.7, 104.8, 53.3 (*C*Me), 4.10 (NMe) and 25.0 (C*Me*).

References

1 B. F. Levine, *Chem. Phys. Lett.*, 1976, **37**, 516.
2 J. L. Oudar and D. S. Chemla, *J. Chem. Phys.*, 1977, **66**, 2664.
3 A. Dulcic and C. Sauteret, *J. Chem. Phys.*, 1978, **69**, 3453.
4 L.-T. Cheng, W. Tam, G. R. Meredith, G. L. J. A. Rikken and E. W. Meijer, *Proc. SPIE*, 1990, **1147**, 61.
5 L.-T. Cheng, W. Tam, S. H. Stevenson, G. R. Meredith, G. Rikken and S. R. Marder, *J. Phys. Chem.*, 1991, **95**, 10631.
6 L.-T. Cheng, W. Tam, S. R. Marder, A. E. Stiegman, G. Rikken and C. W. Spangler, *J. Phys. Chem.*, 1991, **95**, 10643.
7 S. R. Marder, D. N. Beratan and L.-T. Cheng, *Science*, 1991, **252**, 103.
8 S. R. Marder, C. B. Gorman, B. G. Tiemann and L.-T. Cheng, *J. Am. Chem. Soc.*, 1993, **115**, 3006.
9 S. M. Risser, D. N. Beratan and S. R. Marder, *J. Am. Chem. Soc.*, 1993, **115**, 7719.
10 M. Blanchard-Desce, J.-M. Lehn, M. Barzoukas, I. Ledoux and J. Zyss, *Chem. Phys.*, 1994, **181**, 281.
11 S. R. Marder, L.-T. Cheng, B. G. Tiemann, A. C. Friedli, M. Blanchard-Desce, J. W. Perry and J. Skindøj, *Science*, 1994, **263**, 511.
12 A. Dulcic, C. Flytzanis, C. L. Tang, D. Pépin, M. Fétizon and Y. Hoppilliard, *J. Chem. Phys.*, 1981, **74**, 1559.
13 P. N. Prasad and D. J. Williams, *Introduction to Nonlinear Optical Effects in Molecules and Polymers*, Wiley, New York, 1991.
14 D. R. Kanis, M. A. Ratner and T. J. Marks, *Chem. Rev.*, 1994, **94**, 195.
15 M. Barzoukas, A. Fort, G. Klein, A. Boeglin, C. Serbutoviez, L. Oswald and J. F. Nicoud, *Chem. Phys.*, 1991, **153**, 457.
16 M. Barzoukas, A. Fort, G. Klein, C. Serbutoviez, L. Oswald and J. F. Nicoud, *Chem. Phys.*, 1992, **164**, 395.
17 P. C. Leung, J. Stevens, R. E. Harelstad, M. S. Spiering, D. J. Gerbi, C. V. Francis, J. E. Trend, G. V. D. Tiers, G. T. Boyd, D. A. Ender and R. C. Williams, *Proc SPIE*, 1989, **1147**, 48.
18 I. Cabrera, O. Althoff, H.-T. Man and H. N. Yoon, *Adv. Mater.*, 1994, **6**, 43.
19 C. A. van Walree, O. Franssen, A. W. Marsman, M. C. Flipse and L. W. Jenneskens, *J. Chem. Soc., Perkin Trans. 2*, preceding article.
20 M. A. El-Bayoumi, M. El-Aasser and F. Abdel-Halim, *J. Am. Chem. Soc.*, 1971, **93**, 586.
21 M. El-Aasser, F. Abdel-Halim and M. A. El-Bayoumi, *J. Am. Chem. Soc.*, 1971, **93**, 590.
22 M. Adachi, Y. Murata and S. Nakamura, *J. Am. Chem. Soc.*, 1993, **115**, 4331.
23 M. Adachi, Y. Murata and S. Nakamura, *J. Org. Chem.*, 1993, **58**, 5238.
24 E. Haselbach and E. Heilbronner, *Helv. Chim. Acta*, 1968, **51**, 16.
25 J. O. Morley, *J Mol. Struct.* (*Theochem*), 1995, **340**, 45.

26 R. Akaba, H. Sakuragi and K. Tokumaru, *Bull. Chem. Soc. Jpn.*, 1985, **58**, 1186.
27 R. Akaba, H. Sakuragi and K. Tokumaru, *Bull. Chem. Soc. Jpn.*, 1985, **58**, 1711.
28 P. Skrabal, J. Steiger and H. Zollinger, *Helv. Chim. Acta*, 1975, **58**, 800.
29 J. O. Morley, *J. Chem. Soc., Perkin Trans. 2*, 1995, 731.
30 R. Akaba, K. Tokamaru and T. Kobayashi, *Bull. Chem. Soc. Jpn.*, 1980, **53**, 1993.
31 H. Nakai, M. Shiro, K. Ezumi, S. Sakata and T. Kubota, *Acta Crystallogr. Sect. B.*, 1976, **32**, 1827.
32 E. M. Graham, V. M. Miskowski, J. W. Perry, D. R. Coulter, A. E. Stiegman, W. P. Schaefer and R. E. Marsh, *J. Am. Chem. Soc.*, 1989, **111**, 8771.
33 H. H. Jaffé and M. Orchin, *Theory and Applications of Ultraviolet Spectroscopy*, Wiley, New York, 1962, ch. 15.
34 R. Akaba, H. Sakuragi and K. Tokumaru, *Bull. Chem. Soc. Jpn.*, 1985, 301.
35 L. N. Patnaik and S. Das, *Bull. Chem. Soc. Jpn.*, 1987, **60**, 4421.
36 G. Casalone, A. Gavezzotti and M. Simonetta, *J. Chem. Soc., Perkin Trans. 2*, 1973, 342.
37 V. Bertolasi, V. Feretti, P. Gilli and P. G. de Benedetti, *J. Chem. Soc., Perkin Trans. 2*, 1993, 213.
38 E. W. Meijer and E. E. Havinga, *Synth. Met.*, 1993, **57**, 4010.
39 E. W. Meijer and B. L. Feringa, *Mol. Cryst. Liq. Cryst.*, 1993, **235**, 169.
40 R. A Huijts and G. L. J. Hesselink, *Chem. Phys. Lett.*, 1989, **156**, 209.
41 B. F. Levine and C. G. Bethea, *J. Chem. Phys.*, 1975, **63**, 2666.
42 J. L. Oudar, *J. Chem. Phys.*, 1977, **67**, 446.
43 A. L. McClellan, *Tables of Experimental Dipole Moments*, Freeman, San Francisco, 1963.
44 E. Hertel and M. Schinzel, *Z. Physik. Chem.*, 1941, **B48**, 289.
45 J. Dachbach, D. Blackwood, J. W. Pons and S. Pons, *J. Electroanal. Chem.*, 1987, **237**, 269.
46 J. J. P. Steward, MOPAC, version 6.0, QCPE program 504, 1990.
47 A. L. Spek, *J. Appl. Crystallogr.*, 1988, **21**, 578.
48 G. M. Sheldrick, SHELXS86 Program for crystal structure determination, University of Göttingen, Germany, 1986.
49 *International Tables for Crystallography*, ed. A. J. C. Wilson, Kluwer Academic, Dordrecht, 1992, vol. C.
50 G. M. Sheldrick, SHELXL93 Program for crystal structure refinement, University of Göttingen, Germany, 1993.
51 A. L. Spek, *Acta Crystallogr., Sect. A*, 1990, **46**, C34.
52 H.-L. Pan and T. L. Fletcher, *J. Org. Chem.*, 1962, **27**, 3639.
53 D. Vorländer, *Ber.*, 1925, **58**, 1911.
54 *Organikum*, VEB, Berlin, 1981, p. 481.
55 D. D. Perrin, L. F. Armarego and D. R. Perrin, *Purification of Laboratory Chemicals*, Pergamon, Oxford, 1980.
56 D. F. Carson and F. G. Mann, *J. Chem. Soc.*, 1965, 5819.
57 S. Hünig and W. Baron, *Chem. Ber.*, 1957, **90**, 395.
58 J. D. Riedel, GP 80843/1895.
59 H. Franzen and B. von Fürst, *Liebigs Ann. Chem.*, 1917, **412**, 35.
60 E. Enders, in *Houben-Weyl Methoden der organischen Chemie*, Thieme, Stuttgart, 1967, vol. X/2, p. 201.

Paper 6/04609F
Received 2*nd July* 1996
Accepted 19*th November* 1996